PHILOSOPHICAL TRANSACTIONS OF THE ROYAL SOCIETY B BIOLOGICAL SCIENCES

Water-Solute Coupling and Ion Selectivity in Epithelia

Jared M. Diamond

Phil. Trans. R. Soc. Lond. B 1971 **262**, 141-151
doi: 10.1098/rstb.1971.0085

Phil. Trans. Roy. Soc. Lond. B. **262**, 141–151 (1971) [141]
Printed in Great Britain

Water–solute coupling and ion selectivity in epithelia

By Jared M. Diamond
Department of Physiology, University of California Medical Center, Los Angeles, California 90024, *U.S.A.*

[Plate 25]

Water transport across epithelia results from local osmotic gradients set up within the epithelium by active solute transport. These gradients arise in long, narrow, dead-end channels, which function as standing-gradient flow systems. Mathematical analysis of a simple model of such a flow system suggests that the ultrastructural geometry of epithelia accounts for the principal features of water-to-solute coupling. 'Backwards' channels are expected to differ from 'forwards' channels in being hypotonic rather than hypertonic, in their capacity for osmotic filtration, and in being restricted to the active transport of major plasma constituents.

Epithelial pumps and other biological systems distinguish remarkably between closely similar ions, such as Na^+ and K^+, Cl^- and I^-, and Ca^{2+} and Mg^{2+}. Qualitative regularities in discrimination, the so-called selectivity sequences, and quantitative regularities, the so-called selectivity isotherms, make it possible to predict the potencies of untested ions in a given biological system, once the relative effects of two related ions are known for that system. The observed selectivity sequences for the principal inorganic ions of biological interest have been correctly reconstructed by comparing the ions' hydration energies with their interaction energies with membrane sites of different strengths. Details of the selectivity isotherms may provide information about the molecular structure of the biological sites.

This paper summarizes the present status of our attempts to understand two general problems in epithelial function: the mechanism by which water transport is coupled to active solute transport, and the mechanism of ion discrimination.

Coupling of water transport to active solute transport

A principal function of most epithelia is the formation of specialized secretions or absorbates. The driving force for fluid transport is the active transport of specific solutes, often ions, with water accompanying the solute transport as a passive, secondary consequence (Diamond 1962). The coupling does not depend on the building-up, by the solute pump, of external osmotic gradients between the bloodstream and the free epithelial surface, since such gradients are usually non-existent and most epithelia can transport water not only in the absence of, but even against, external osmotic gradients. However, osmosis at some local level within the epithelium must be involved (Diamond 1964), since the transported fluid has been shown to be isosmotic to the bathing solution regardless of the latter's absolute osmolarity in the gall-bladder, intestine, pancreas and Malpighian tubule. It turns out that the coupling mechanism is intimately related to the ultrastructural geometry of the transporting epithelium.

Figure 1, plate 25, is an electron micrograph of rabbit gall-bladder, an epithelium that transports an isotonic NaCl solution from its luminal surface to its blood surface in order to concentrate bile. The salient anatomical features include an array of microvilli at the luminal surface; numerous mitochondria, particularly near the luminal surface; and the lateral intercellular paces, a system of long, narrow, dead-end channels which are open towards the bloodstream

but are closed at the luminal surface by so-called tight junctions (Kaye, Wheeler, Whitlock, & Lane 1966; Tormey & Diamond 1967). At these tight junctions the membranes from adjacent cells fuse to form complete hoops around the base of each barrel-shaped cell, sealing off the lumen from the lateral spaces. In combined physiological and anatomical experiments J. Tormey and I showed that the lateral spaces were distended by about 1 μm during maximal fluid transport but collapsed down to 20 nm or less when fluid transport was inhibited by any means. Series of control experiments showed that these changes did not result from changes in cell

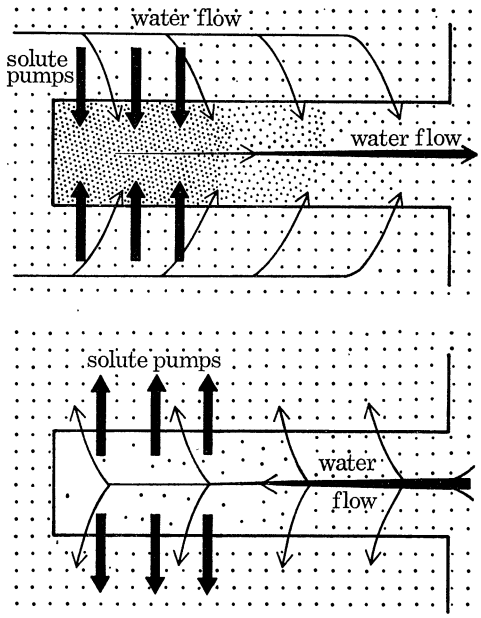

FIGURE 2. Comparison of 'forwards' and 'backwards' operation of a standing-gradient flow system, which consists of a long narrow channel closed at one end (e.g. a basal infolding, lateral intercellular space, etc.). The density of dots indicates the solute concentration. Forwards operation (top): solute is actively transported into the channel across its walls, making the channel fluid hypertonic. As solute diffuses down its concentration gradient towards the open mouth, more and more water enters the channel across its walls due to the osmotic gradient. In the steady state a standing osmotic gradient will be maintained in the channel by active solute transport, with the osmolarity decreasing progressively from the closed end to the open end; and a fluid of fixed osmolarity (isotonic or hypertonic, depending upon the values of such parameters as radius, length, and water permeability) will constantly emerge from the mouth. Backwards operation (bottom): solute is actively transported out of the channel across its walls, making the channel fluid hypotonic. As solute diffuses down its concentration gradient towards the closed end, more and more water leaves the channel across its walls owing to the osmotic gradient. In the steady state a standing osmotic gradient will be maintained in the channel by active solute transport, with the osmolarity decreasing progressively from the open end to the closed end; and a fluid of fixed osmolarity (isotonic or hypertonic, depending upon the parameters of the system) will constantly enter the channel mouth and be secreted across its walls. Solute pumps are depicted only at the bottom of the channels for illustrative purposes but may have different distributions along the channel. (From Diamond & Bossert 1968.)

volume, changes in muscle tone, or fixation artefacts, and that the lateral spaces constituted the route of fluid transport (Diamond & Tormey 1966*a*, *b*). Evidently NaCl is continually being actively pumped from the cells into the lateral spaces, making them hypertonic, and it is within these spaces that the local osmotic gradients responsible for water-to-solute coupling are developed.

Virtually all fluid-transporting epithelia are characterized by some structures—lateral spaces, basal infoldings, or intracellular canaliculi—that conform to this geometry of long, narrow,

dead-end channels (e.g. gall-bladder, vertebrate intestine, renal proximal and distal tubule, ciliary body, salivary gland striated duct, choroid plexus, liver, pancreas, stomach; see articles in this volume on frogskin by Ussing (p. 85) on Malpighian tubule by Maddrell (p. 197), on insect rectum by Ramsay (p. 251) on cephalopods by Denton (p. 277), and on avian salt gland by Peaker (p. 289). In several other epithelia, as in the gall-bladder, such channels have been shown to constitute the route of fluid transport. The way in which this shared geometrical ground-plan couples water transport to solute transport is illustrated in the top of figure 2. As solute is dumped into the channel and diffuses down its concentration gradient towards the open mouth of the channel, water enters osmotically across the channel walls, progressively reducing the osmolarity. In the steady state the channel contents will be hypertonic, a standing osmotic gradient will be maintained along the length of the channel by active solute transport, and a fluid of constant osmolarity—isotonic or hypertonic, depending on factors such as the geometry and water permeability—will continually emerge from the mouth of this standing-gradient flow system. The progressive approach to osmotic equilibrium along the channel accounts for the maintenance of water flow despite the complete absence of osmotic gradients between the final secretion or absorbate and the bathing solution (Diamond 1971).

From analysis of diffusion and convection in the channel W. Bossert and I derived the differential equation describing this flow system:

$$N(x)+\frac{Dr^2}{4P}\frac{\mathrm{d}^3v}{\mathrm{d}x^3}-\frac{r^2v}{4P}\frac{\mathrm{d}^2v}{\mathrm{d}x^2}-\frac{C_0r}{2}\frac{\mathrm{d}v}{\mathrm{d}x}\frac{r^2}{4P}\left(\frac{\mathrm{d}v}{\mathrm{d}x}\right)^2=0, \tag{1}$$

where the independent variables are the channel length L, the radius r, the water permeability of the channel walls P, the solute diffusion coefficient D, the distance x from the closed end of the channel, the bathing solution osmolarity C_0, and the rate of active solute transport across its walls $N(x)$ (Diamond & Bossert 1967). The dependent variables are the osmolarity of the fluid inside the channel $C(x)$ and the linear velocity of water flow from the closed to the open end of the channel $v(x)$. Using ranges of values of the independent variables actually found in epithelia. Bossert and I solved this differential equation by computer for the osmolarity of the fluid continually emerging from the open mouth in the steady state, given by the expression

$$2\pi r\int_{x=0}^{x=L}N(x)\,\mathrm{d}x\Big/\pi r^2v(L).$$

We found that the predicted transported osmolarities ranged from isotonic up to a few times isotonic, i.e. the range of values actually encountered in epithelia. As illustrated in figure 3, the form of the calculated standing gradients is that the osmolarity of the channel fluid decreases from maximally hypertonic at the closed end towards isotonic at the open end. As an example of how the effects of changes in the values of the independent variables on the transported osmolarity may be calculated, figure 4 gives the transported osmolarity as a function of the solute transport site. The transported fluid is most nearly isotonic when all the solute is dumped in at the closed end of the channel, and becomes progressively hypertonic (the magnitude of the hypertonicity depending on other parameters such as the water permeability) as the solute pump is spread over an increasing fraction of the channel length, because the distance to the channel mouth is then shorter and there is less opportunity for osmotic equilibration. This relation may explain why the mitochondria in the gall-bladder are concentrated towards the closed end of the channel, if we may assume that the distribution of the energy sources is a clue to the distribution of the pumps. One may similarly show that the transported fluid is more

nearly isotonic, the higher the water permeability of the channel walls or the longer or narrower the channel. The transported osmolarity is predicted to be virtually independent of the transport rate, even for epithelia with values of the independent variables such that the transported fluid is hypertonic—in agreement with experimental findings for the avian salt gland and the distal tubule. The point should be stressed that the transported osmolarity is determined by several

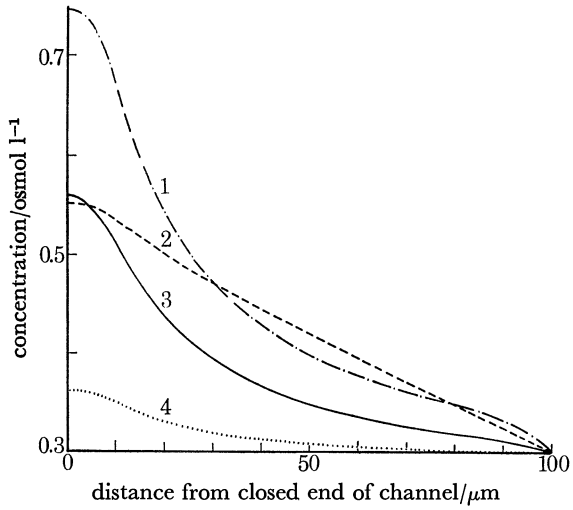

FIGURE 3. Examples of concentration profiles in a standing-gradient flow system, calculated from equation (1). The solute concentration in the channel in the steady-state (ordinate) is plotted against x, the linear distance from the closed end of the channel (abscissa). The following values were chosen for the independent variables of equation (1): the length L was held fixed at 100 μm, the radius r at 0.05 μm, the bathing concentration C_0 at 0.3 osmol/l, and the diffusion coefficient D at 10^{-5} cm^2/s; the solute transport rate N was held at 10^{-5} (curve 1) 5×10^{-6} (curve 3), or 10^{-6} (curves 2 and 4) mosmol cm^{-2} s^{-1} for $0 < x < 10$ μm, and at zero for $x > 10$ μm; the water permeability P was held at 2×10^{-5} (curves 1, 3 and 4) or 1×10^{-6} (curve 2) cm s^{-1} osmol^{-1}. Note that the solute concentration in the channel decreases from a maximally hypertonic value at the closed end towards isotonic (0.30 osmol/l) at the open end. The corresponding calculated concentrations of the emergent fluid (equation (2)) were 0.342 (curve 1), 0.803 (curve 2), 0.318 (curve 3), and 0.304 (curve 4) osmol/l. (From Diamond & Bossert 1967.)

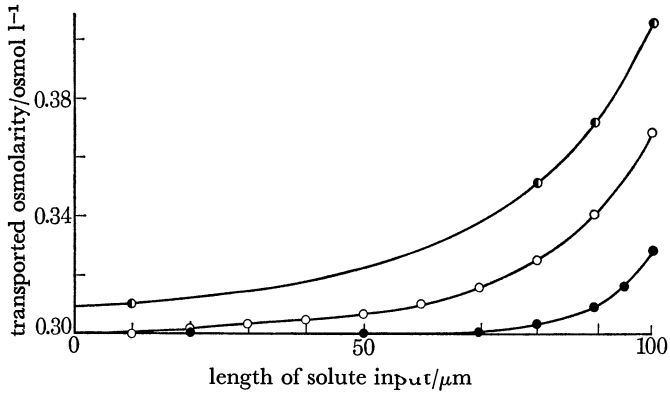

FIGURE 4. The effect of varying solute transport site upon the osmolarity of fluid produced by a backwards standing-gradient flow system, calculated from equation (1). L was held at 100 μm, r at 0.05 μm, C_0 at 0.3 osmol/l, D at 10^{-5} cm^2/s, and P at 1×10^{-5} (◐), 2×10^{-5} (○), or 1×10^{-4} (●) cm s^{-1} osmol^{-1}. A given solute transport rate (N) held over a range of x from zero (the closed end of the channel) out to the value given on the abscissa, and N was zero for x greater than this value. The transport rate for the whole channel was held fixed at $-(2\pi rL)$ (10^{-7}) mosmol/s, by choosing N (transport rate per unit wall area, in mosmol cm^{-2} s^{-1}) as $-(100)$ (10^{-7}) divided by the length of solute input in micrometre. Note that the transported fluid is most nearly isotonic (0.3 osmol/l) when solute input is confined towards the closed end of the channel, and becomes progressively hypertonic as solute transport extends over an increasing fraction of the channel length. (From Diamond & Bossert 1968.)

PHILOSOPHICAL TRANSACTIONS OF THE ROYAL SOCIETY B BIOLOGICAL SCIENCES

factors and therefore cannot be predicted from knowledge of one variable alone. For instance, if epithelium *a* is observed to have shorter channels than epithelium *b*, it does not necessarily follow that *a* will have a more hypertonic transported fluid than *b*, since the two epithelia may also differ in other respects such as water permeability and transport site.

This reconstruction applies to epithelia where the channels are oriented such that fluid transport is from the closed to the open end. This is the situation in many epithelia, including gall-bladder, vertebrate intestine and kidney. In some other epithelia, such as choroid plexus, avian salt gland, and Malpighian tubule, the anatomy is 'backwards'—i.e. fluid transport is in the direction from the open to the closed end of the channel (Diamond & Bossert 1968). As illustrated in the lower half of figure 2, solute is probably being pumped out of rather than into the channels of these 'backwards' epithelia: the channel goes hypotonic, water is absorbed out of the channel and flows into its open mouth, and standing gradients are established such that the channel osmolarity progressively decreases from the open to the closed end. Calculation shows, however, that the transported fluid is still isotonic or hypertonic, as observed experimentally in 'backwards' epithelia, and that effects of changes in the independent variables on the transported osmolarity are as in 'forwards' epithelia. 'Backwards' epithelia are predicted to differ from 'forwards' epithelia in two respects. First, 'backwards' epithelia can develop effective gradients only if the actively transported solute is a major constituent of plasma. In agreement with this theoretical restriction, most of the known 'backwards' epithelia secrete NaCl or other major plasma constituents, while epithelia secreting trace constituents of plasma (e.g. the stomach and the liver, secreting HCl and bile salts, respectively) have 'forwards' channels. Second, the anatomy of 'backwards' epithelia makes them ideally suited for an osmotic filtration mechanism in which active transport of one solute sweeps along any permeant solute. All plasma constituents are carried into the open mouth of the channel and accumulate at the closed end at raised concentrations, favouring passive diffusion across the epithelium. Osmotic filtration does actually make conspicuous contributions to fluid secretion in two 'backwards' epithelia, Malpighian tubule and choroid plexus.

Within the last year it has been demonstrated experimentally in three epithelia with 'forwards' channels that the postulated hypertonicity of the channels does exist. T. Machen and I (Machen & Diamond 1969) used an indirect electrical method in rabbit gall-bladder, taking advantage of the fact that this epithelium is preferentially permeable to cations, so that the dilute bathing solution goes electrically positive when a salt concentration gradient is present across the gall-bladder. If the lateral spaces do contain a raised NaCl concentration during maximal fluid transport, this local concentration gradient across the epithelium should set up a diffusion potential (luminal solution electrically positive to the lateral spaces). We were able to detect this predicted local diffusion potential, and from its magnitude we estimated that the lateral spaces were on the average hypertonic by 20 mosmol/l. In insect rectum the channels are large enough that Wall (1971) was able to sample their contents with micropipets and demonstrate hypertonicity by direct analysis. Finally, Swanson & Solomon (1970) obtained micropuncture samples from various points along the pancreatic duct and demonstrated not only that the fluid is hypertonic but that the osmolarity decreases in a standing gradient along the length of the duct.

Several questions concerning standing osmotic gradients remain unresolved. We are only beginning to get experimental estimates of their magnitudes. If standing gradients in the lateral spaces account for water movement from gall-bladder epithelial cells to the bloodstream, it

PHILOSOPHICAL TRANSACTIONS OF THE ROYAL SOCIETY B BIOLOGICAL SCIENCES

is not clear where the gradients are that make water move from the gall-bladder lumen into the cells. Standing gradients in the microvilli are one possibility, but an alternative suggested by Lindemann (1968) is that the operation of the solute pump and standing gradients at the lateral membrane may make the cell contents anisotonic and create an osmotic gradient across the whole luminal cell membrane. Finally, P. Barry, E. Wright, and I found that the high-conductance pathway for passive transepithelial ion permeation in the gall-bladder is across the tight junctions rather than across the cells (Barry, Diamond, & Wright 1971), and we do not know whether some water as well flows directly across the tight junctions, though sequential equilibration along the lateral spaces via the cells would still be essential for obtaining an isotonic transported fluid.

We can summarize our present understanding of water–solute coupling in epithelia as follows. Water transport across epithelia is coupled to active solute transport by means of local osmotic gradients set up within the epithelium. These gradients are located in subcellular structures with a distinctive geometry, namely, long and narrow dead-end channels, which function as standing-gradient flow systems. Analysis of a simple model of such a system suggests that it can account for the main features of water-solute coupling in epithelia, such as fluid transport in the complete absence of external osmotic gradients, the range of osmolarities transported, and the relation between transported osmolarity and solute transport rate. 'Backwards' channels are predicted to differ from 'forwards' channels in being hypotonic rather than hypertonic, in their capcity for osmotic filtration, and in being restricted to the active transport of major plasma constituents. Thus, water–solute coupling to epithelia may be a geometrical consequence of epithelial ultrastructure.

Ion selectivity

The other general feature of epithelial function that I shall discuss is the problem of ion selectivity. Most epithelia possess highly specific Na^+ pumps, while a few possess highly specific K^+ pumps. The large differences these pumps exhibit in their affinities for the five alkali cations (Li^+, Na^+, K^+, Rb^+, Cs^+) are remarkable when one considers how similar are the physical properties of the alkali cations, which may be approximated as rigid, non-polarizable spheres with modest differences in radius (ionic radii Li^+ 60 pm, Na^+ 95 pm, K^+ 133 pm, Rb^+ 148 pm, Cs^+ 169 pm). Alkali cation discrimination is equally important in many other processes, such as the permeability changes underlying electrical excitation in nerve, muscle, synapses, and sense organs, the activation and inhibition of enzymes, the maintenance of cell resting potentials, and the selectivity of glass electrodes. All these processes exhibit such striking qualitative regularities in cation discrimination, the so-called selectivity sequences, and such striking quantitative regularities, the so-called selectivity isotherms, as to suggest that a common mechanism of selectivity underlies these diverse processes. There are equally striking specificities and regularities in anion discrimination, examples including the Cl^- pumps of the stomach and of fish gill, I^- accumulation by the thyroid gland, and HCO_3^- secretion by pancreas. Similar regularities appear in specific effects of the alkaline-earth cations, Ca^{2+}, Mg^{2+}, Sr^{2+} and Ba^{2+}. It is now possible to predict many ion affinities semi-quantitatively from the selectivity isotherms and to reconstruct the observed selectivity sequences from simple physical principles. As an example of this approach, pioneered by Eisenman (1961, 1965), I shall discuss the reconstruction of the selectivity sequences for the halide anions, but the same approach suffices to predict Na^+ to K^+ discrimination and Ca^{2+} to Mg^{2+} discrimination.

PHILOSOPHICAL TRANSACTIONS OF THE ROYAL SOCIETY B BIOLOGICAL SCIENCES

The four halide anions are qualitatively similar in their physical and chemical properties, and the quantitative differences that exist arise from their differences in radius (ionic radii: F^- 136 pm, Cl^- 181 pm, Br^- 195 pm, I^- 216 pm). Many pumps and other biological processes nevertheless discriminate markedly among the halides. As the starting-point of our analysis, let us look for regularities in this discrimination, noting that four ions can be permuted on paper to form 4! or 24 different combinations. In fact, 17 of these combinations have yet to be recorded as the selectivity sequence for any biological process, and the remaining seven sequences are observed again and again in nature (Diamond & Wright 1969). These seven observed sequences, listing the most permeant or most potent ion at the top in each case, are:

1	2	3	4	5	6	7
I^-	Br^-	Br^-	Cl^-	Cl^-	Cl^-	F^-
Br^-	I^-	Cl^-	Br^-	Br^-	F^-	Cl^-
Cl^-	Cl^-	I^-	I^-	F^-	Br^-	Br^-
F^-	F^-	F^-	F^-	I^-	I^-	I^-

For instance, sequence 1 is the permeability sequence in rabbit gall-bladder, and the affinity sequence of the I^- pump in thyroid gland; sequence 3 is the permeability sequence for the outer surface of bullfrog skin; and sequence 5 is the permeability sequence for erythrocytes. Note that sequence 7 is the inverse sequence of the ionic radii, sequence 1 is the reverse of this sequence and each adjacent pair of sequences differs only in the inverted positions of one anion pair. The inversions begin (from sequence 1) with the inversion of the largest anions, I^- and Br^-, proceed through inversions of the next largest anion, Cl^- (sequences 2 to 4), and end (sequences 4 to 7) with inversions of the smallest anion, F^-. In addition, there are quantitative regularities in biological selectivity patterns, such that a given sequence is associated only with a certain range of potency or permeability ratios. E. Wright and I utilized these regularities to construct the selectivity isotherms of figure 5, which plot the relative potency ratios for a given biological system as a function of the I^+/Cl^- ratio for that system. The relative potencies of F^- and Br^- do not scatter at random but cluster around clearly defined curves, indicating that the F^- and Br^- potencies are systematic functions of the I^-/Cl^- potency ratio. From these empirical isotherms, if one measures the effects of any two halides in a biological system, one can predict not only the whole halide sequence, but also, semi-quantitatively, the effects of the other two halides.

What is the explanation of these regularities? On energetic grounds, one expects that an anion in a biological membrane will generally have some positively charged atom (probably N or H) as its nearest neighbour, while the anion's nearest neighbour in water will be the positive end of a water molecule, i.e. the hydrogen. In physicochemical terms, the anion with the strongest affinity for a membrane site (e.g. for an active transport pump) will be that anion which experiences the largest free-energy decrease when its environment becomes the site rather than water. That is, the equilibrium binding constant for transfer of the anion from water to the site is governed by the free-energy difference

$$\Delta F_{\text{transfer}} = \Delta F_{\text{ion-site}} - \Delta F_{\text{ion-water}}$$

where $\Delta F_{\text{ion-site}}$ is the free energy of anion-site interaction and $\Delta F_{\text{ion-water}}$ is the anions' free energy of hydration. Let us re-express this in pictorial terms: transferring an ion from water to a membrane site requires work to tear the ion out of water but yields energy as the ion is attracted to the site. The preferred ion will be the one which yields the most energy or else requires the

PHILOSOPHICAL TRANSACTIONS OF THE ROYAL SOCIETY B BIOLOGICAL SCIENCES

least work for the net transfer process. In the extreme case of a very strong site (e.g. one with a high positive charge), ion-site interaction energies greatly exceed hydration energies; the smallest anion, F^-, has the highest value of $\Delta F_{\text{ion-site}}$, since its centre of charge is nearest the site at the distance of closest approach; and the binding sequence is simply the inverse sequence of ionic radii, $F^- > Cl^- > Br^- > I^-$, sequence 7. In the other extreme case of a very weak site (e.g. one with a small positive charge) such that hydration energies greatly exceed the values of

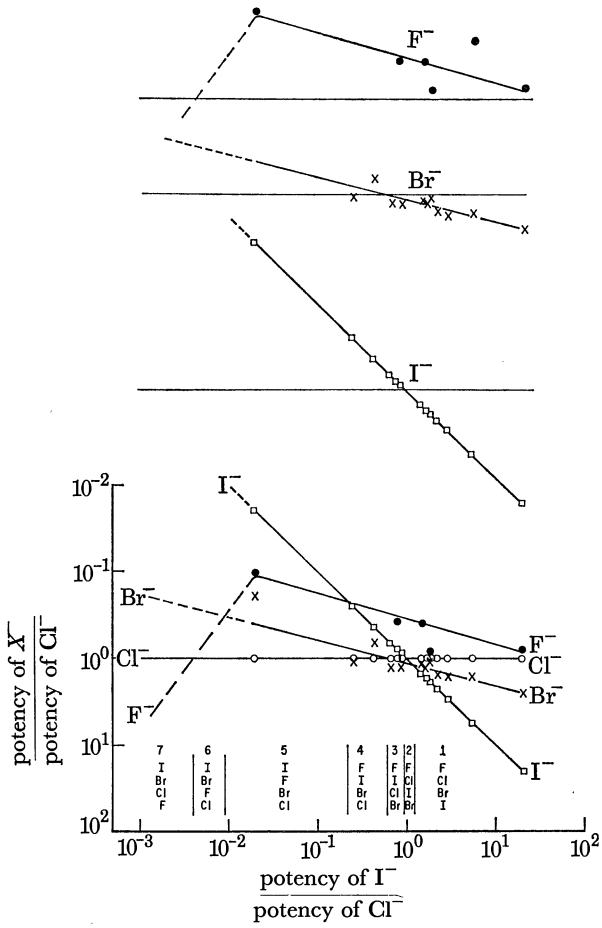

FIGURE 5. Below, selectivity isotherms for the halide anions in biological systems. Each set of four points arranged vertically above each other is a relative potency sequence experimentally measured in a biological system. (●, F^-; ○, Cl; ×, Br^-; □, I^-). The potencies relative to $Cl^- = 1$ are plotted logarithmically on the ordinate. They are arranged according to the relative I^- potency, plotted logarithmically on the abscissa. [For instance, halides inhibit the enzyme carbonic anhydrase with the relative potencies $I^- = 22.2$, $Br^- = 2.5$, $Cl^- = 1.0$, $F^- = 0.8$. These points have therefore been arranged on an imaginary vertical line intersecting the horizontal axis at 22.2, and constitute the set of points lying furthest to the right. Since the ordinate gives potency relative to Cl^- as a function of the relative I^- potency on the abscissa, the Cl^- value of 1.0 automatically falls on a horizontal line intersecting the ordinate at 1.0, and the I^- value of 22.2 automatically falls on the line of 45° slope. The Br^- value of 2.5 and the F^- value of 0.8 have been used in constructing the empirical isotherms for these two ions, drawn by eye through all the Br^- or F^- points.] The intersections of these four experimental isotherms represent transitions among seven sequences predicted theoretically as shown in Figure 6 and listed below the pattern and numbered 1 to 7 (the most potent ion is written at the bottom in each case). Above, the F^-, Br^-, and I^- isotherms are replotted separately for clarity. The meaning of the regular pattern is that once the relative potencies of two halides are known, the whole sequence and the approximate potencies of the other two halides can be predicted. For instance, reading vertically upwards from 0.1 on the abscissa, a system in which I^- is one tenth as potent as Cl^- should be in sequence 5 ($Cl^- > Br^- > F^- > I^-$) and should have a F^- potency of about 0.2 and a Br^- potency of about 0.6 relative to Cl^-. (From Diamond & Wright 1969.)

PHILOSOPHICAL TRANSACTIONS OF THE ROYAL SOCIETY B BIOLOGICAL SCIENCES

$\Delta F_{\text{ion-site}}$, the preferred ion is the ion that requires the least work to tear out of water, i.e. the largest anion, I^-, which because of its large size has the lowest hydration energy; and the binding sequence is simply the inverse sequence of hydration energies, $I^- > Br^- > Cl^- > F^-$, sequence 1.

In order to calculate the remaining sequences expected for intermediate site strengths, we need some method of approximating $\Delta F_{\text{ion-site}}$, energies of hydration already being known experimentally. The simplest approach would be to apply Coulomb's law to calculate the

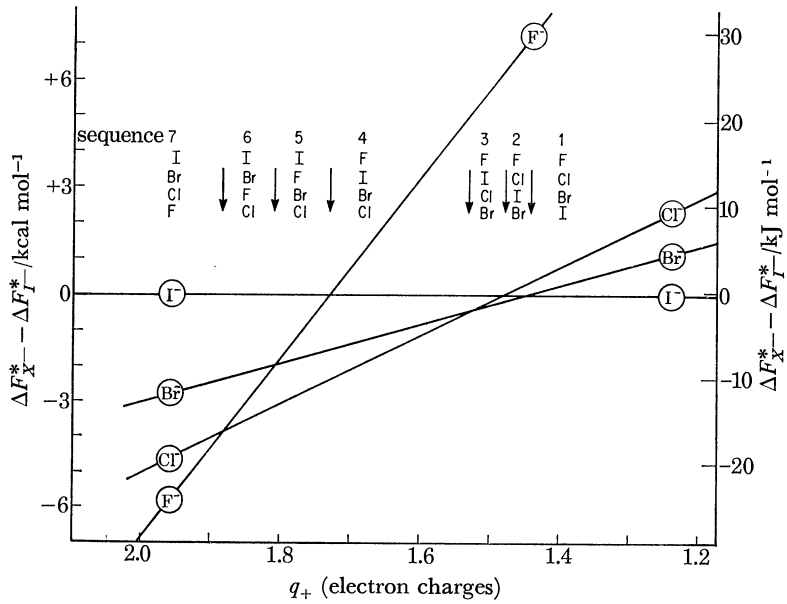

FIGURE 6. Prediction of halide selectivity sequences in biological systems. The attraction between a halide anion and a positive membrane site is approximated by the Coulomb expression $(q_-)\,(q_+)/(r_+ + r_-)$ where q_- or q_+ is the charge and r_- or r_+ the radius of the halide and the site, respectively. The free-energy change in transferring a halide from water to the site, written as ΔF^* or $\Delta F_{\text{transfer}}$, is given by the difference between this Coulomb expression and the halide's free energy of hydration. The ordinates give this calculated ΔF^* for each halide minus ΔF^* for I^-, as a function of the site charge q_+. The Pauling ionic radii were used for r_-, the Latimer hydration energies for $\Delta F_{\text{hydration}}$, q_- is one electron charge, and r_+ was arbitrarily taken as 0.15 nm, the van der Waals's radius of nitrogen. At any given value of q_+, the anion with the most negative ΔF^* is the most potent anion. Intersections between two curves, as indicated by vertical arrows, correspond to cross-over points between different selectivity sequences, read off on the graph from the relative positions of the curves (the most potent ion on the bottom). The seven sequences thus determined are the same as those that occur in biological systems (written on p. 147 with the most potent ion on top).

attraction between each halide anion and a positive site of fixed radius, carrying out the calculation for various values of the site charge. As illustrated in figure 6, subtraction of $\Delta F_{\text{ion-water}}$ from these Coulomb values of $\Delta F_{\text{ion-site}}$ yields curves of $\Delta F_{\text{transfer}}$ for each anion as a function of site strength. The curves intersect each other six times, the intersections determining transitions from one selectivity sequence to another. It will be seen that the seven resulting predicted sequences are the same as the ones observed experimentally in biological systems. The same results have been obtained by several other methods of modelling $\Delta F_{\text{ion-site}}$, such as applying Coulomb's law to a site of fixed charge but varying radius, or using the alkali cations as site models and equating $\Delta F_{\text{ion-site}}$ with experimental values of crystal lattice energies or diatomic gas dissociation energies of the alkali halides.

Thus, a simple treatment in which Coulomb's law is used to approximate the forces between

PHILOSOPHICAL TRANSACTIONS OF THE ROYAL SOCIETY B BIOLOGICAL SCIENCES

anions and membrane sites, and in which these Coulomb forces are balanced against hydration energies, suffices to predict selectivity patterns of the halides in all biological systems studied to date. The implication is that what gives different pumps or membranes different anion specificities is differences in the strength of positively charged binding sites.

Identical considerations apply to discrimination among the alkali cations, except that these will be associated with negative rather than positive membrane sites (probably oxygen atoms). Eisenman (1965) showed that 11 of the 120 possible permutations of the five alkali cations recur as biological selectivity sequences, and that these are correctly predicted by a Coulomb model. These 11 Coulomb sequences, listing the most potent ion on top in each case, are:

1	2	3	4	5	6	7	8	9	10	11
Cs	Rb	Rb	K	K	K	Na	Na	Na	Na	Li
Rb	Cs	K	Rb	Rb	Na	K	K	K	Li	Na
K	K	Cs	Cs	Na	Rb	Rb	Rb	Li	K	K
Na	Na	Na	Na	Cs	Cs	Cs	Li	Rb	Rb	Rb
Li	Li	Li	Li	Li	Li	Li	Cs	Cs	Cs	Cs

For instance, permeation in rabbit intestine fits sequence 1, permeation in frog intestine fits sequence 2, permeation in frog gall-bladder fits sequence 3, the 'potassium pump' in Malpighian tubules of *Calliphora* fits sequence 4, the resting potential of squid axon fits sequence 4 or 5 (depending on the particular squid used), and the 'sodium pump' of beef cornea and the action potential of squid axon fit sequence 11. Sequence 11 is the inverse sequence of ionic radii; sequence 1 is the inverse sequence of hydration energies; each adjacent pair of sequences differs only in the inverted positions of one cation pair; and the inversions begin (from sequence 1) with the inversion of the largest cations, Cs^+ and Rb^+, proceed through inversions of the next largest cation, K^+ (sequences 2 to 4), then the next largest cation, Na^+ (sequences 4 to 7), and end (sequences 7 to 11) with inversions of the smallest cation, Li^+.

In regard to the alkaline-earth cations (Mg^{2+}, Ca^{2+}, Sr^{2+}, Ba^{2+}), Wright and I showed (Diamond & Wright 1969) that only seven of the 24 possible permutations commonly occur as biological selectivity sequences, and that these were the sequences predicted by Sherry (1969) from a Coulomb model and by me from the crystal lattice energies of the oxide, sulfide, and selenide crystals of these cations. These sequences, listing the most potent ion on top in each case, are:

1	2	3	4	5	6	7
Ba	Ba	Ca	Ca	Ca	Ca	Mg
Sr	Ca	Ba	Ba	Mg	Mg	Ca
Ca	Sr	Sr	Mg	Ba	Sr	Sr
Mg	Mg	Mg	Sr	Sr	Ba	Ba

For instance, effects of alkaline-earth cations on permselectivity in the gall-bladder fit sequence 3, permeability of erythrocytes fits sequence 4, and maintenance of permselectivity in the intestine fits sequence 7. Sequence 7 is the inverse sequence of ionic radii, while sequence 1 is the inverse sequence of hydration energies.

Finally, selectivity isotherms can also be constructed for more complex ions, such as the polyatomic monovalent anions ClO_4^-, SCN^-, NO_3^- and ClO_3^- (J. M. Diamond, unpublished observations).

Study of ion selectivity is now at a stage where fine details of the selectivity isotherms in a

group of tissues may permit conclusions about the molecular structure of the site. For instance, there are systematic quantitative differences between the alkali cation selectivity isotherms in epithelia and in the membranes of single cells such as nerve and muscle: the epithelial isotherms show a smaller spread, and the Li^+ isotherm is shifted downwards. The physical meaning of these differences is that in epithelia the permeation route is more hydrated (as inferred from the smaller spread of the isotherms), and the sites are more polarizable (as inferred from the Li^+ shift), than in single cells (Barry *et al.* 1971: figure 7).

Summarizing this brief survey of ion selectivity, one can say that epithelial pumps and other biological systems discriminate remarkably between closely similar ions, such as Na^+ and K^+, Cl^- and I^-, and Ca^{2+} and Mg^{2+}. Within each group of ions there are qualitative regularities, such that only a few of the possible ion permutations exist in nature as selectivity sequences. There are also quantitative regularities expressed in the selectivity isotherms, that permit the prediction of ion effects once one knows the relative effects of any two ions of a given group in a given biological system. In the cases of the halide anions, the alkali cations, and the alkaline-earth cations, the observed sequences have been correctly predicted by comparing the ions' hydration energies with their Coulomb interaction energies with membrane positive or negative sites. Tissues or pumps that yield different selectivity sequences do so because they differ with respect to their site strength. From fine details of selectivity patterns it may be possible to draw some conclusions about the molecular structure of the sites.

The work reported here was supported in part by NIH grant no. GM-14772 and NIH programme project grant no. HE-11351.

References (Diamond)

Barry, P. H., Diamond, J. M. & Wright, E. M. 1971 *J. Membrane Biol.* **4**, 358.
Diamond, J. M. 1962 *J. Physiol., Lond.* **161**, 474.
Diamond, J. M. 1964 *J. gen. Physiol.* **48**, 15.
Diamond, J. M. 1971 *Fedn. Proc. Fedn Am. Socs exp. Biol.* **30**, 6.
Diamond, J. M. & Bossert, W. H. 1967 *J. gen. Physiol.* **50**, 2061.
Diamond, J. M. & Bossert, W. H. 1968 *J. Cell Biol.* **37**, 694.
Diamond, J. M. & Wright, E. M. 1969 *A. Rev. Physiol.* **31**, 581.
Diamond, J. M. & Tormey, J. M. 1966*a* *Nature, Lond.* **210**, 817.
Diamond, J. M. & Tormey, J. M. 1966*b* *Fedn. Proc. Fedn. Am. Socs exp. Biol.* **25**, 1458.
Eisenman, G. 1961 In *Symposium on membrane transport and metabolism* (eds. A. Kleinzeller and A. Kotyk), p. 163. New York: Academic Press.
Eisenman, G. 1965 In *Proc. 23rd Int. Congr. Physiol. Sci., Tokyo*, p, 489. Amsterdam: Excerpta Medical Foundation.
Kaye, G. I., Wheeler, H. O., Whitlock, R. T. & Lane, N. 1966 *J. Cell Biol.* **30**, 237.
Lindemann, B. 1968 Habilitation Thesis, Universität des Saarlandes.
Machen, T. E. & Diamond, J. M. 1969 *J. Membrane Biol.* **1**, 194.
Sherry, H. S. 1969 In *Ion exchange*, vol. 2 (J. A. Marinsky, ed.), p. 89. New York: Dekker.
Swanson, C. H. & Solomon, A. K. 1970 *Fedn. Proc. Fedn. Am. Socs exp. Biol.* **29**, 845 Abstr.
Tormey, J. M. & Diamond, J. M. 1967 *J. gen. Physiol.* **50**, 2031.
Wall, B. 1971 *Fedn. Proc. Fedn Am. Socs exp. Biol.* (in the Press).

PHILOSOPHICAL TRANSACTIONS OF THE ROYAL SOCIETY B BIOLOGICAL SCIENCES